AIP | Applied Physics Letters

Inductive pulsed phase thermography for reducing or enlarging the effect of surface emissivity variation

Ruizhen Yang, Yunze He, Bin Gao, and Gui Yun Tian

Citation: Applied Physics Letters **105**, 184103 (2014); doi: 10.1063/1.4901531
View online: http://dx.doi.org/10.1063/1.4901531
View Table of Contents: http://scitation.aip.org/content/aip/journal/apl/105/18?ver=pdfcov
Published by the AIP Publishing

Articles you may be interested in

Transient thermography testing of unpainted thermal barrier coating surfaces
AIP Conf. Proc. **1511**, 571 (2013); 10.1063/1.4789098

Irradiance-based emissivity correction in infrared thermography for electronic applications
Rev. Sci. Instrum. **82**, 114901 (2011); 10.1063/1.3657154

Emissivity-corrected power loss calibration for lock-in thermography measurements on silicon solar cells
J. Appl. Phys. **103**, 113503 (2008); 10.1063/1.2930880

Progress in phase angle thermography
Rev. Sci. Instrum. **74**, 417 (2003); 10.1063/1.1524010

Pulsed thermography modeling
AIP Conf. Proc. **615**, 564 (2002); 10.1063/1.1472848

This article is copyrighted as indicated in the article. Reuse of AIP content is subject to the terms at: http://scitation.aip.org/termsconditions. Downloaded to IP: 125.71.229.163 On: Thu, 20 Nov 2014 02:30:53

APPLIED PHYSICS LETTERS **105**, 184103 (2014)

Inductive pulsed phase thermography for reducing or enlarging the effect of surface emissivity variation

Ruizhen Yang,[1,a)] Yunze He,[2,b)] Bin Gao,[3] and Gui Yun Tian[3,4]
[1]*Department of Civil Engineering, Changsha University, Changsha 410022, People's Republic of China*
[2]*College of Mechatronics Engineering and Automation, National University of Defense Technology, Changsha 410073, People's Republic of China*
[3]*School of Automation Engineering, University of Electronic Science and Technology of China, Chengdu 610054, People's Republic of China*
[4]*School of Electrical and Electronic Engineering, Newcastle University, Newcastle upon Tyne, NE1 7RU, United Kingdom*

(Received 11 October 2014; accepted 30 October 2014; published online 7 November 2014)

Emissivity variation introduces illusory temperature inhomogeneity and results in false alarms in infrared thermography, thus, it is important to separate the influence of surface emissivity variation. This letter experimentally demonstrates the advantages of phase information to reduce or enlarge the effect of surface emissivity variation with inductive pulsed phase thermography, where inductive excitation is emissivity-independent and avoids the effect of emissivity variation in heating process. The directly heated area and the indirectly heated area are divided in the phasegrams. The emissivity variation is removed or enlarged perfectly at the specific frequency and defect detectability is improved remarkably. © *2014 AIP Publishing LLC*.
[http://dx.doi.org/10.1063/1.4901531]

Infrared (IR) thermography based on diffusion wave fields is a non-contact and non-destructive measurement and detection technique with an increasing span of applications.[1–3] Inductive thermography is an emerging IR thermography for conductive material, which combines the advantages of eddy current testing and IR thermography such as non-contact, fast, and high resolution.[4,5] In previous works, inductive thermography has been used for damage detection in metallic alloy[6] and carbon fibre reinforced plastic.[7,8] Defects were indicated by a high/low temperature spots in the 2D thermograms. In the *in-situ* application, the materials under test (MUT) always have oil, coating, or an oxidation layer on the surface, which changes the thermal emissivity significantly. The variation can be used to detect the surface damage like rust or corrosion.[9] However, the variation sometimes introduces illusory temperature, inhomogeneity, and results in false alarms.[10] To remove or separate the influence of surface emissivity variation in IR, thermography testing is important and several methods have been attempted in previous studies. The first is spraying water or black paint on aluminium samples to eliminate high reflectance and raise emissivity.[11] The method can improve the homogeneity of the surface emissivity, however, water or black paint not only pollutes the sample but also increases the cost and complexity of the test procedure. The second is the logarithmic analysis based on the 1D heat conduction. Shepard proposed thermographic signal reconstruction (TSR) to reduce the influence of low thermal emissivity.[12] The third is the normalization technique. Lugin normalized the temperature curves based on thermal equilibrium to compare quantitative evolutions of the curves.[13] The last but not the least is the phase information by using a Fourier transformation, which attracts a widely applications in flash thermography,[14] lock-in thermography,[15] and pulse phase thermography.[16] In addition, Mandelis proposed an emissivity-normalized, higher-dynamic-range contrast parameter known as cross-correlation phase in thermal-wave radar (TWR).[1,17] Speaking of inductive thermography, inductive excitation is an emissivity-independent way of subsurface heating depending on the induction frequency and the electrical properties of MUT, which remove the effect of emissivity variation in heating process. Yang and He proposed the logarithmic analysis of temperature response for steel detection but did not mention the separation of emissivity variation.[18] Bai *et al*. proposed a two heat balance states-based normalization method to remove the influence of surface emissivity variation.[10] Gao *et al*. proposed a non-negative pattern separation model to automatically extract large differences in surface emissivity.[19] However, the phase information has not been applied to remove or enlarge the emissivity variation in inductive thermography. Combining eddy current excitation, infrared imaging and phase analysis, inductive pulsed phase thermography (IPPT) technique was proposed in previous work[20] and used to quantify the subsurface defects.[21] This letter proposed phase information in IPPT to reduce or enlarge the effect of emissivity variation and experimental studies were presented to validate the proposed method.

The basic principle of IPPT has been provided in previous work.[20] A small period of high frequency current is driven to generate the resistive heat in the conductive material. Consequently, the surface temperature distribution is captured by IR camera and the sequence of infrared images is transmitted to PC. For each pixel, the temperature sequence is normalized by the following equation:[10,13]

$$T_{\mathrm{norm}}(t) = \frac{T(t) - T(t_0)}{T(t_1) - T(t_0)}, \tag{1}$$

a)Electronic mail: xbaiyang@163.com. Tel.: +86731 84261208.
b)Electronic mail: hejicker@163.com. Tel.:+8613467698133.

 © 2014 AIP Publishing LLC

This article is copyrighted as indicated in the article. Reuse of AIP content is subject to the terms at: http://scitation.aip.org/termsconditions. Downloaded to IP: 125.71.229.163 On: Thu, 20 Nov 2014 02:30:53

where $T(t)$ is the temperature at the time t, $T(t_0)$ and $T(t_1)$ are the temperatures at the beginning of heating (frame 1) and at the end of temperature sequence, respectively. And then, the Discrete Fourier Transform (DFT) is computed for each temperature responses according to the well-known formula

$$F(f) = \Delta t \sum_{n=0}^{N-1} T(n\Delta t) e^{-i2\pi f n \Delta t} = R(f) + iI(f), \qquad (2)$$

where Δt is the sampling time step, $R(f)$ and $I(f)$ are, respectively, the real and imaginary components of $F(f)$. Then, the phase spectra are computed using the following equation:

$$\varphi(f) = \tan^{-1}\left[\frac{I(f)}{R(f)}\right]. \qquad (3)$$

At last, the phases at some specific frequency are extracted from phase spectra and to construct the 2D phasegrams, which can be used to indicate the defects by abnormal area.

The developed IPPT system is shown in previous work.[20] An Easyheat 224 from Cheltenham Induction Heating is used for coil excitation, which has a maximum excitation power of 2.4 kW, a maximum current of $400\mathrm{A_{rms}}$, and an excitation frequency range of 150−400 kHz. A rectangular coil is constructed from 6.35 mm high-conductivity hollow copper tube. Water is pumped through the coil during operation to aid in cooling. The IR camera is Flir SC7500, which is a Stirling cooled camera with a 320×256 array of 1.5–5 μm InSb detectors. This camera has a sensitivity of <20 mK and a maximum full frame rate of 383 Hz. A PC is used to implement the DFT.

A steel sample ($0.24 \times 45 \times 100\,\mathrm{mm^3}$) with a slot of 10 mm length, 2 mm width was prepared, as shown in Fig. 1(a). Thermal conductivity of the stainless steel is $14\,\mathrm{Wm^{-1}\,K^{-1}}$. There are equally spaced shinning and black stripes with 5 mm width on the sample surface. The shinning strips are the polished area, while the black strips are the area sprayed with black painting. They illustrate different emissivity. The emissivity of the black region is 1, which is the same for a blackbody. While, the emissivity of the shinning stainless steel surface is about 0.16. The inductive excitation is an emissivity-independent way of sub-surface heating depending on the induction frequency and the electrical properties (conductivity and permeability) of MUT.

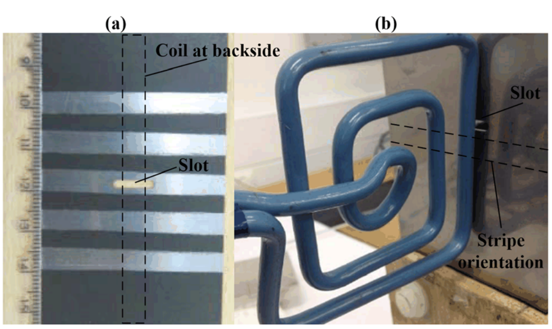

FIG. 1. (a) Steel sample with slot; (b) relative position of coil and steel sample.

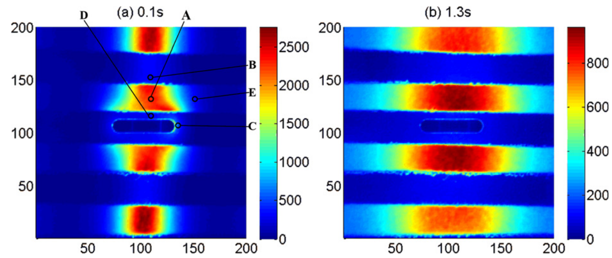

FIG. 2. Original thermograms at (a) 0.1 s and (b) 1.3 s.

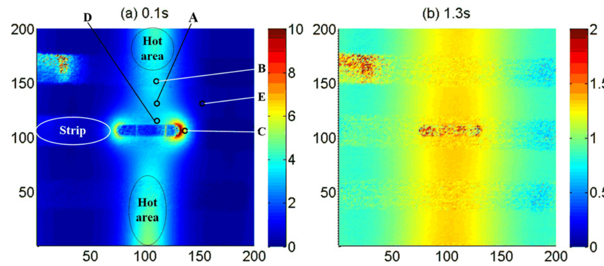

FIG. 3. Thermograms after normalization at (a) 0.1 s and (b) 1.3 s.

Ferromagnetic metals with high permeability have a much smaller skin depth (about 0.04 mm at 100 kHz and 0.03 mm at 200 kHz).[20] Thus, the emissivity variation on the sample does not affect heating process. In the experiments, coil and IR camera were placed on the opposite side, presenting transmission mode.[8] The coil was perpendicular to the slot and across the slot centre. Only one edge of the rectangular coil was used to stimulate eddy current in the sample, as shown in Fig. 1(b). A 0.1 s heating duration was selected for inspection, which was long enough to elicit an observable heat pattern. The cooling time after heating was 1.9 s, which was long enough to ensure the sample reaching a new thermal equilibrium state. The total recorded time was 2 s, and the sampling frequency was 383 Hz.

During inductive thermography testing, when an eddy current encounters a discontinuity, e.g., a slot or a notch, they are forced to divert, leading to areas of increased and decreased eddy current density resulting in relatively hotter and cooler areas due to Joule heating. Fig. 2(a) shows the thermogram at the end of heating (0.1 s). Due to the high emissivity of the black area, there is no obvious high temperature region around the slot tips. The high temperature can

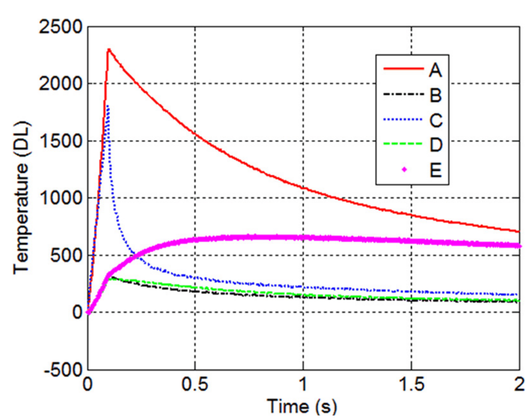

FIG. 4. Original transient responses for different positions.

This article is copyrighted as indicated in the article. Reuse of AIP content is subject to the terms at: http://scitation.aip.org/termsconditions. Downloaded to IP: 125.71.229.163 On: Thu, 20 Nov 2014 02:30:53

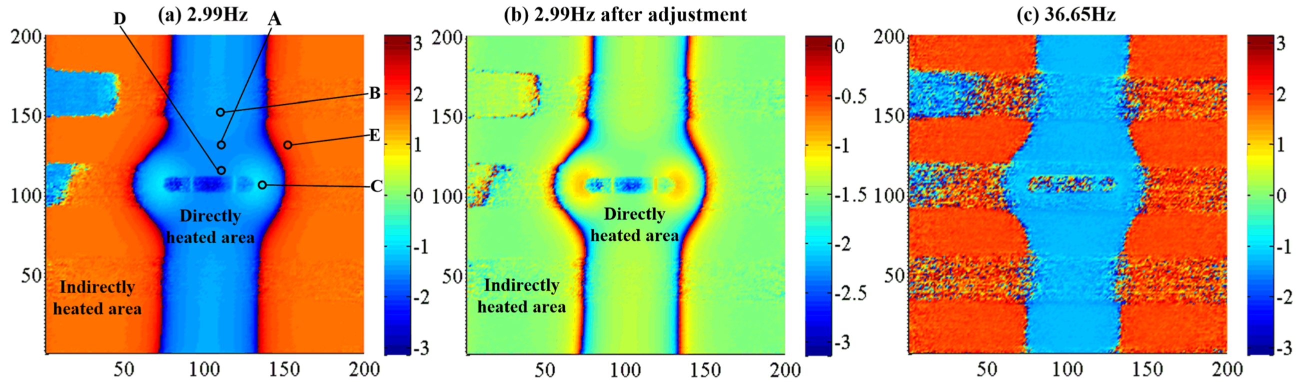

FIG. 5. (a) Phasegram at 2.99 Hz; (b) phasegram after adjustment at 2.99 Hz; and (c) phasegram at 36.65 Hz.

only be observed at the black area above the coil. In addition, Fig. 2(b) shows the thermogram at the cooling phase (1.3 s). The high temperature still can only be observed at the black strip area because of both high emissivity and heat diffusion.

The method known as normalization technique was evaluated first.[10] By setting t_1 as 2 s, all transient responses were normalized using Eq. (1). The corrected thermograms at 0.1 s and 1.3 s are shown in Figs. 3(a) and 3(b), respectively. Comparing with thermograms in Fig. 2, the black stripes were reduced but still can be observed, especially in Fig. 3(b). And the hot temperature area directly heated by coil is still interference for identifying the defects. This means that the non-uniform heating is there. The results using non-negative pattern separation model can be found out in previous work.[19] The same problem can be observed.

The transient temperature response at different positions is shown in Fig. 4. As marked in Figs. 2(a) and 3(a), point A is at the defect-free area with black strip (high emissivity), point B at the defect-free area with shinning strip (low emissivity), point C is at the crack tip with the shinning strip, point D is at the crack side with shinning strip above the coil, and point E is at the black strip where the area is far away from the excitation. The transient response at point C is four times higher than that at point B at the end of heating, which is indicative of the crack. However, because of high emissivity, the transient response at point A is also several times higher than at point B. Therefore, due to emissivity variation, hot spots cannot be taken as an indicator of defects.

Using the IPPT, all transient responses in cooling phase were processed using Eqs. (2) and (3), and the phasegrams at specific frequency were obtained. Fig. 5(a) presents the phasegram at 2.99 Hz. The black stripes are almost invisible. Point C at the tip of defect has the highest temperature, whereas point D at the defect side has the lowest temperature. These are in line with the results in the previous works.[22–24] The related phase spectra for five points are shown in Fig. 6(a). Obviously, phase spectra for point C are different from that for point B, especially at the low frequency from 0 to 20 Hz. It is noticed that instead of a large difference between the transient responses of point A and point B in Fig. 4, the two responses are roughly approximated in Fig. 6(a). This demonstrates that the influence of surface emissivity variation is removed. In addition, the phase spectra for point E are obviously different from point A, although they are on the same defect-free area with black strip. The reason is that point A is at the heat source area, which is directly heated by eddy current, while point E is at the area where heat is obtained from lateral heat conduction, as marked in Fig. 5(a). This phenomenon can be observed from Fig. 4. The temperature response for point E arrives at its maximal value at 0.8 s but not 0.1 s. In other words, the temperature response for the directly heated area is a decreasing process after 0.1 s, while for the indirectly heated area there is a rising process after 0.1 s. Therefore, temperature responses for points A and E are in a counter trend move (anti-phase). We can find from Fig. 6(a) that the phase spectra for point E are greater than point A by exact one π (3.14). If we subtract 3.14 from phase spectra for point E, their spectra are similar, as shown in Fig. 6(b). Fig. 5(b) shows the phasegram after adjustment at 2.99 Hz. As the same in Fig. 5(a), there is an obvious boundary between

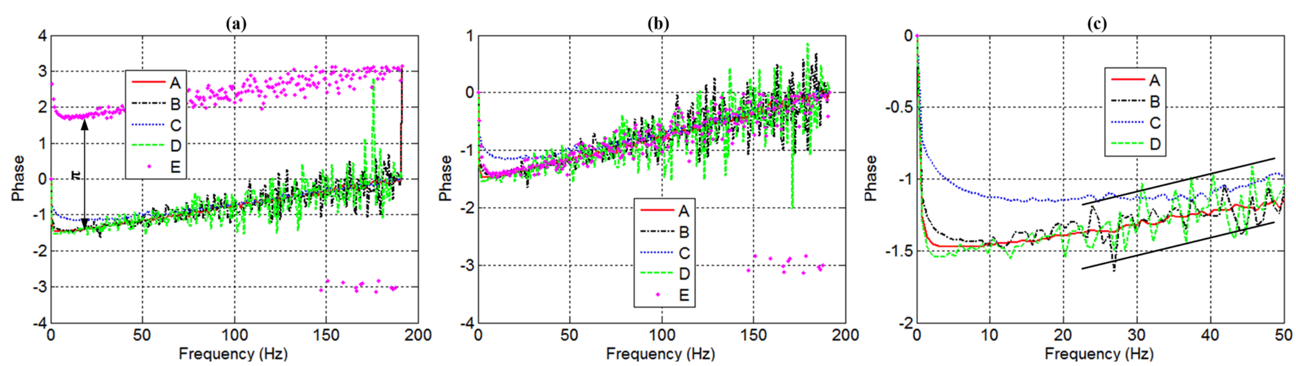

FIG. 6. (a) Phase spectra for five points; (b) phase spectra after adjustment for five points; and (c) phase spectra for four points from 0 to 50 Hz.

This article is copyrighted as indicated in the article. Reuse of AIP content is subject to the terms at: http://scitation.aip.org/termsconditions. Downloaded to IP: 125.71.229.163 On: Thu, 20 Nov 2014 02:30:53

directly heated area and indirectly heated area. In Figs. 5(a) and 5(b), the emissivity variation can be removed in directly heated area or indirectly heated area. And the non-uniform heating can also be removed. This is an immerse improvement and the defect area could be identified more accurately in directly heated area. In previous work,[21] the subsurface defect area could be identified in indirectly heated area. Thus, the ability of reducing emissivity variation means that the detectability of both surface defect and subsurface defect will be improved remarkably.

Fig. 6(c) shows the phase spectra for four points from 0 to 50 Hz. The phase spectra for point C are biggest and that for point D are smallest at low frequency. There trends are agreed with the previous results.[22–24] After 25 Hz, the phase spectra for points B and D at the directly heated area of polished strip present great fluctuations, while phase spectra for point A at the directly heated area of black strip area have small fluctuations. This indicates that the phasegram at relative high frequency can be used to show the variation of emissivity between polished and black strips. Fig. 5(c) shows the phasegram at 36.65 Hz. Obviously, the polished strips with variation of emissivity and defect area are visible. This can be used to detect the corrosion or rust, which makes the emissivity different from material under test.[9]

In this letter, phase information was extracted using IPPT to reduce or enlarge the effect of surface emissivity variation. For each pixel, the phase spectra were obtained by DFT after normalization. A verified experiment was carried out on a steel sample having both polished and black strips. The phasegrams at low frequency were used to remove the emissivity variation, and the phasegrams at relative high frequency were used to enlarge the emissivity variation. The heat of indirectly heated area is from the directly heated area and the temperature responses for these two areas are in an opposite trend (anti-phase), thus their phase spectra have a difference (one π). There is an obvious boundary between these two areas in the phasegrams. The emissivity variation can be perfectly removed in directly heated area or indirectly heated area. The experimental results showed that image quality was improved significantly, which is particularly useful to indicate the defect correctly.

The work was supported by National Natural Science Foundation of China (Grant Nos. 51377015 and 51408071).

[1] N. Tabatabaei, A. Mandelis, and B. T. Amaechi, Appl. Phys. Lett. **98**(16), 163706 (2011).
[2] F. Fertig, J. Greulich, and S. Rein, Appl. Phys. Lett. **104**(20), 201111 (2014).
[3] A. Mandelis, L. Nicolaides, and Y. Chen, Phys. Rev. Lett. **87**(2), 020801 (2001).
[4] Y. He, M. Pan, D. Chen, G. Tian, and H. Zhang, Appl. Phys. Lett. **103**(19), 194101 (2013).
[5] A. Yin, B. Gao, G. Yun Tian, W. L. Woo, and K. Li, J. Appl. Phys. **113**(6), 064101 (2013).
[6] Y. He, M. Pan, and F. Luo, Rev. Sci. Instrum. **83**, 104702 (2012).
[7] L. Cheng and G. Tian, IEEE Sens. J. **11**(12), 3261–3268 (2011).
[8] Y. He, G. Tian, M. Pan, and D. Chen, Compos. Struct. **109**, 1–7 (2014).
[9] Y. He, G. Tian, M. Pan, D. Chen, and H. Zhang, Corros. Sci. **78**, 1–6 (2014).
[10] L. Bai, S. Tian, Y. Cheng, G. Y. Tian, Y. Chen, and K. Chen, IEEE Sens. J. **14**(4), 1137–1142 (2014).
[11] N. P. Avdelidis and D. P. Almond, Infrared Phys. Technol. **45**(2), 103–114 (2004).
[12] S. M. Shepard, in *IV Pan American Conference for Non Destructive Testing* (Buenos Aires, Argentina, 2007).
[13] S. Lugin, NDT&E Int. **56**, 48–55 (2013).
[14] J.-C. Krapez, L. Spagnolo, M. Frieß, H.-P. Maier, and G. Neuer, Int. J. Therm. Sci. **43**(10), 967–977 (2004).
[15] K. Chatterjee and S. Tuli, IEEE Trans. Instrum. Meas. **61**(4), 1079–1089 (2012).
[16] X. Maldague and S. Marinetti, J. Appl. Phys. **79**(5), 2694–2698 (1996).
[17] N. Tabatabaei and A. Mandelis, Phys. Rev. Lett. **107**(16), 165901 (2011).
[18] R. Yang and Y. He, Infrared Phys. Technol. **67**, 467–472 (2014).
[19] B. Gao, L. Bai, W. L. Woo, and G. Tian, Appl. Phys. Lett. **104**(25), 251902 (2014).
[20] Y. He, G. Tian, M. Pan, and D. Chen, Appl. Phys. Lett. **103**(8), 084104 (2013).
[21] Y. He, M. Pan, G. Tian, D. Chen, Y. Tang, and H. Zhang, Appl. Phys. Lett. **103**(14), 144108 (2013).
[22] J. Wilson, G. Y. Tian, I. Z. Abidin, S. Yang, and D. Almond, Nondestr. Test. Eval. **25**(3), 205–218 (2010).
[23] L. Bai, B. Gao, G. Y. Tian, W. L. Woo, and Y. Cheng, IEEE Sens. J. **13**(6), 2094–2101 (2013).
[24] B. Gao, L. Bai, W. L. Woo, G. Y. Tian, and Y. Cheng, IEEE Trans. Instrum. Meas. **63**(4), 913–922 (2014).

This article is copyrighted as indicated in the article. Reuse of AIP content is subject to the terms at: http://scitation.aip.org/termsconditions. Downloaded to IP: 125.71.229.163 On: Thu, 20 Nov 2014 02:30:53